

## STEEL MECHANICAL PROPERTIES EVALUATED AT ROOM TEMPERATURE AFTER BEING SUBMITTED AT FIRE CONDITIONS

Piloto, P.A.G.<sup>1</sup>; Vila Real, Paulo<sup>2</sup>; Mesquita, Luís<sup>3</sup>; Vaz, M.A.P.<sup>4</sup>

<sup>1,3</sup> Applied Mechanics department, Polytechnic Institute of Bragança, Ap. 1134, 5301-857 Bragança, Portugal  
e-mails: [ppiloto@ipb.pt](mailto:ppiloto@ipb.pt); [imesquita@ipb.pt](mailto:imesquita@ipb.pt)

<sup>2</sup> Civil department, University of Aveiro, Campus Santiago, 3810 Aveiro  
e-mail: [pvreal@civil.ua.pt](mailto:pvreal@civil.ua.pt)

<sup>4</sup> Mechanical department, Engineering Faculty - University of Porto, Rua Dr. Roberto Frias S/N  
e-mail: [gmavaz@fe.up.pt](mailto:gmavaz@fe.up.pt)

**Key words:** mechanical properties, fire conditions, residual stress relief, metallurgic phase transformation

### Abstract

Several researchers have already studied the effect of temperature increase in steel structures regarding load-bearing capacity and some material models have been developed in fire conditions, based on experimental results. The mechanical properties of a S275 JR steel construction material has been tested at elevated temperatures after a natural and forced cooling. The major focus has been made on yield and ultimate strength behavior, hardness material and residual stress relief. Experimental results will be presented for each temperature level, dwell time and cooling rate. Test results were compared with the normal room temperature condition. The material specimens were cutted from the web of each unit length IPE 100 profiles, after being heated by means of electro ceramic mat resistance and tested at the universal machine, according to NP EN 10002-1 standard. Microstructure analysis has been done regarding each different steel state, based on the standard NP-1467. The hardness tests has been determined for some steel specimen conditions over the entire cross section, according to NP 4072 standard. The results shown that material yield strength from the tested heated specimens are smaller and grater when compared with the yield strength of the used material at room temperature, depending on the temperature level during fire and respective cooling rate. Residual stresses were measured as closed as possible to ASTM E837-01. A stress relief was thermally induced and the final stress state measured and compared with the initial state.

## 1 Introduction

For steel structures under high temperature the relationship between stress and strain changes considerably. At high temperature, the material properties degrade and its capacity to deform increases, which is measured by the reduction of the Young's modulus [1]. Basic material research of structural steel materials is becoming more important as the significance of fire engineering design of steel structures is growing and new steel materials, including high-strength steels and stainless steels are going to be used more widely in steel structures in the near future [2,3].

The load bearing capacity after fire conditions mainly depends on the fire duration, critical temperature and on the cooling process phase. The structural material behaviour will be very important, regarding its mechanical properties after being subjected to metallurgic transformations.

During fire conditions, the structural material will be charged with high thermal gradients at elevated temperatures that may produce metallurgic transformations, according to the steel equilibrium diagram represented in figure 1. In general, very slow cooling rates from elevated temperatures will follow the iron – iron carbide equilibrium diagram. Any rate of cooling, interpreted as nonequilibrium, should be analysed by using the time – temperature – transformation (TTT) curves [4], as represented in the figure 2.

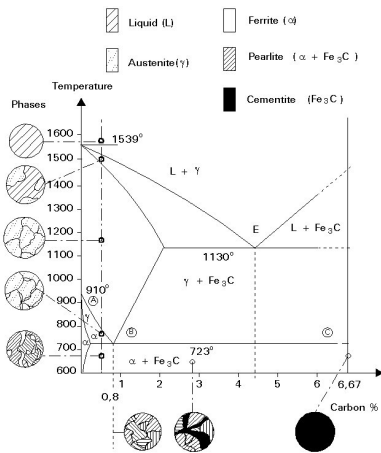


Figure 1: Iron – iron carbide equilibrium diagram [13].

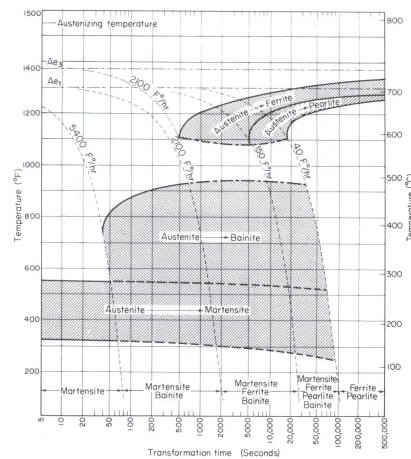


Figure 2: Continuous cooling transformation curve [4].

Lines of different slopes on this diagram can show the effect of the cooling rate. Slow cooling may lead to the formation of pearlite ferrite mixture. Cooling at an intermediate rate passes through pearlite/ferrite transformation at higher temperatures, but changes to bainite transformation at lower temperatures so that a mixture of pearlite and bainite results. A higher rate in the cooling phase may result in phase transformation to martensite after passing through the two horizontal lines. Thus in practice, varying the cooling rate may produce different steel composition and resultant properties [8]. The material under testing is a steel S275 JR with 0.16% carbon, 1.15% Mn, 0.24% Si, 0.008% P, 0.01% S, 0.05% Cr, 0.05% Ni, 0.01% Mo, among other chemical elements, as reported in the inspection certificate from the manufacturer.

## 2 Steel mechanical properties at elevated temperatures

The first models to represent the behavior of steel materials in fire situation used simple methods of calculation. Thus the extrapolation was the only way to represent the difference at elevated temperatures regarding the values at room temperature. The stress – strain relationship used at 20 [°C] and all the other necessary parameters were studied and several values of deformation 0.2%, 0.5% and

2% to represent the yield of the material have been established. The results of Rubert and Schaumann [10] were transposed to the Eurocodes, and they have established a model in which the material creep would be considered in a implicit way.

In the linear elastic range, the Elastic Modulus will change due to the increasing of temperature as can be seen in the figure 3, representing this material property with a reduction coefficient.

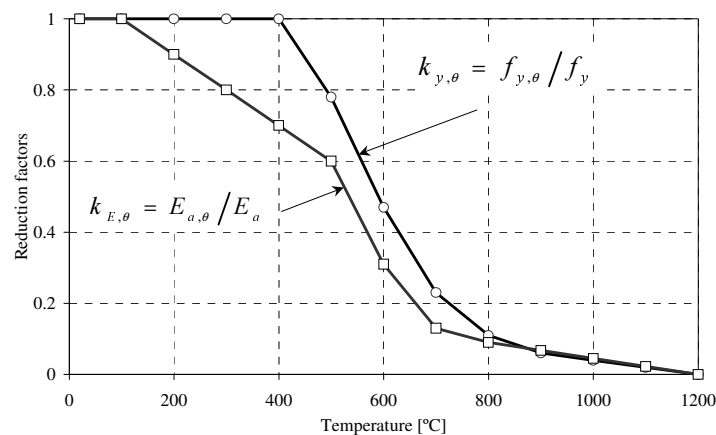


Figure 3: Reduction coefficient for yield strength and for elastic modulus.

This variation is the result of a tabulated relationship between the value of the Elasticity Modulus at elevated temperature and the reference value at room temperature (equation in figure 3) [11].

After several experimental and numerical campaigns, Franssen [12] propose analytical expressions to represent the behavior of yield strength. In Eurocode 3 [11], this mechanical property variation is presented in tabulated data, with a coefficient that references the material property value at high temperature to the value at room temperature (equation in figure 3) [11].

### 3 Experimental procedure

Several specimens were submitted to high different temperature conditions and to different cooling rates (natural cooling and quenching). The mechanical properties have been compared regarding the material strength, HRB and HRC hardness and its metallurgic microstructure. The heating phase was achieved using the electro ceramic mat resistance (see figures 4 and 5), at constant rate equal to 800 [°C/hour]. The temperature was controlled at two different points and the cooling phase controlled by another thermocouple.

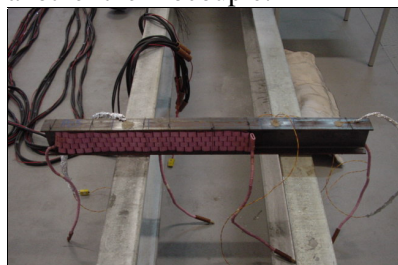


Figure 4: Beam thermocouple instrumentation.



Figure 5: Beam heated at 800 [°C] during one hour.



Figure 6: Beam cooling procedure (quenching).

The cooling procedure varied from natural to forced, as shown in the figure 6. The quenching was done with a water vessel at normal temperature condition. When a metal at high temperature is submerged in a quenching medium, the temperature variation is time dependent, regarding three

distinct phases. First, the water in contact with the piece heats rapidly to its boiling point and converts to steam, forming a film or blanket around the metal and insulates it from the liquid water. As the metal cools, the violent generation of steam subsides and some of the liquid becomes in contact with metal surface, even with boiling going on, promoting a high heat transfer rate. When enough heat is removed, the steel loses the ability to convert the liquid into steam and the liquid cooling stage begins [15].

#### 4 Tensile tests

The process for determining the yield stress has been carried out as closely to code [7]. The specimen has been machined from the web of the steel beam element, has shown in figure 7, according to the dimensions of each specimen.



Figure 7: Samples location and specimens geometry.

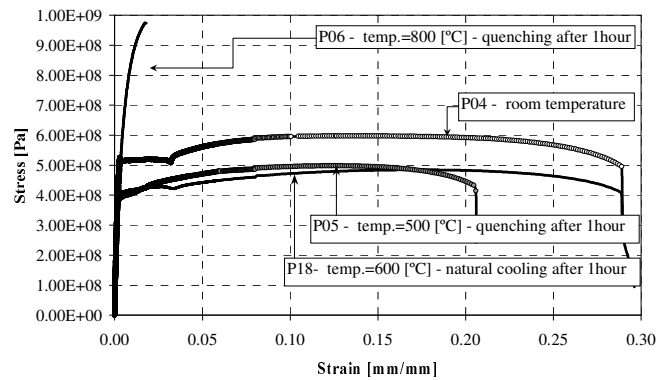


Figure 8: Stress – Strain curve for specimens tested at different conditions.

The speed increment for each part of the stress strain curve has been used according the standard [7]. The specimens were tested on a universal testing 4885 Instron machine with the data acquisition system GPIB assisted by a personal computer. The resultant stress – strain curve are shown in the figure 8, regarding four different material conditions. The yield range has been specially analyzed to present the results in table 1.  $R_m$  represents the ultimate stress while  $R_{eH}$  and  $R_{eL}$  represents the higher and lower yield stress.

Table 1: Tensile test results at room temperature.

Test	$R_{eH}$ [MPa]	$R_{eL}$ [MPa]	$R_m$ [MPa]	$R_{p0.2}$ [MPa]	$A_f$ [%]
P01	492	499	575	492	34.5
P02	511	493	592	507	33.5
P03	507	498	580	505	35.0
P04	525	508	597	518	28.9
Average $\pm$ Sdv	509 $\pm$ 14	500 $\pm$ 6	586 $\pm$ 10	506 $\pm$ 11	33.0 $\pm$ 2.8

In the case of brittle material, the yield stress should be considered equal to  $R_{p0.2}$  and the extension after collapse  $A_f$  will be smaller. Several specimens were heated during 1 hour at each different temperature level followed by quenching. The results are presented in table 2.

Table 2: Tensile test results after being submitted to high temperatures and quenching.

Test	Temperature [°C]	$R$ [MPa]	$R_{p0.2}$ [MPa]	$A_t$ [%]
P05	500	498	391	20.60
P08	500	532	453	25.30
P13	500	552	469	40.00
P16	500	576	493	37.00
P12	600	575	500	24.35
P14	600	506	429	31.00
P15	600	512	382	30.00
P09	700	506	294	22.12
P06	800	974	687	1.74
P07	800	988	717	7.10
P11	800	987	786	9.67
P10	850	1140	758	9.76

Other testing conditions were carried out with the same steel material and with natural cooling rate. The results are presented in the table 3 according to the typical stress strain curves with residual stress relief. The tested specimens P18 and P19 presents yield strength level that is 100 [MPa] smaller than the normal state condition.

Table 3: Results from the tensile tests at several temperatures with natural cooling.

Test	Temperature [°C]	$R$ [MPa]	$R_{p0.2}$ [MPa]	$A_t$ [%]
P17	500	515	482	36.98
P20	500	580	501	36.76
P18	600	485	410	29.61
P19	600	474	390	36.86

The test P17 and P20 could not achieve the transition temperature for stress relieving, producing a standard stress-strain curve.

## 5 Hardness tests

The hardness Rockell B and C was measured over the entire cross section from the top flange till the bottom, passing through the web. The precision in this measuring is in compliance with ISO 716 standard and the method according to ISO 6508 and Portuguese standard NP4072 [5]. The penetrator used for measuring Rockwell B was a ball with 1/16'' diameter, with a preload of 10 [kgf] and a load of 100 [kgf], while for measuring Rockwell C, 120° diamond penetrator was used with the same preload and 150 [kgf] of total force. The time suggested to load and unload the specimen was 6 [s]. The average results of 39 measured points over the entire cross section from the IPE specimens were made for several different conditions, according to the next table.

Table 4: Rocwell B and C hardness results from specimens at different conditions.

Test	Temperature [°C]	Dwell Time [hour]	Water cooling	Hardness HRBm Average $\pm$ Sdv	Hardness HRC Average $\pm$ Sdv
1	20	-	-	92.9 $\pm$ 1.4	-
2	600	1	yes	85.0 $\pm$ 3.2	-
3	600	1	no	81.6 $\pm$ 3.3	-
4	800	1	yes	-	38.6 $\pm$ 2.4
5	850	1	yes	-	40.3 $\pm$ 4.2

The HRB scale was used for measuring hardness for soft steel material while the HRC scale was used for hardened material. The difference between test 2 and 3 is not significant, while maximum hardness results were obtained from steel material that has been submitted to austenithique transformation and high energetic cooling process.

## 6 Metallography analysis

The metallurgical analysis was made at several different state conditions. At room temperature the specimens were cutted from two different zones. Those two specimens were transversally cutted from the IPE 100 cross section and both surface were prepared in three different phases (pre polishing, polishing and chemical attack). In the first phase the specimen must be prepared without scratches and spots. The polishing phased is normally executed by fine abrasives and should produce a specular bright and undeformed microstructure. The chemical attack (nitric acid 5 [cm<sup>3</sup>] plus 100 [cm<sup>3</sup>] of ethylic alcohol) should be used during 30 seconds maximum, in order to obtain a good optical contrast regarding different metal elements, different phases and different orientation in grain size. This procedure was made with reference [6] and in accordance to ASTM E 3-62 and ASTM E 7-63.

At room temperature is possible to see the two-equilibrium phases material (ferrite and pearlite), as expected and represented in the figure 9.

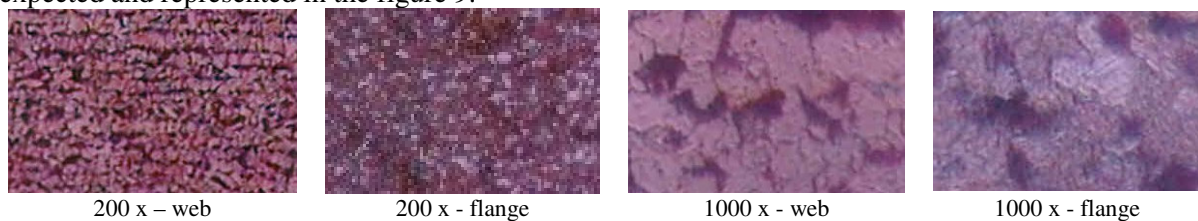


Figure 9: Microstructure from steel in received conditions from the manufacturer.

For the case of a steel heated at 800 [°C] during one hour and with a rapid cooling the microstructure expected will be martensite or eventually bainite, as can be inspected from the figure 10.

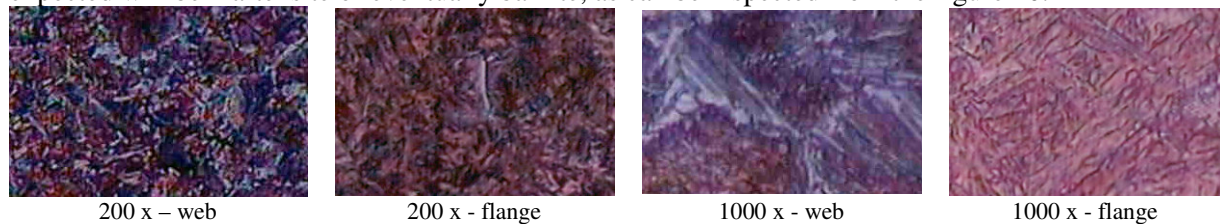


Figure 10: Microstructure from steel after 1 hour at 800 [°C] and quenching cooling.

## 7 Residual stress relief

The magnitude and geometric distribution of the residual stresses may vary with the geometry of the cross section and with the straightening and cooling processes. The idealized distribution is expressed in the figure 11 and will be used to measure the residual stress in a specific point of the beam length.



Figure 11: Residual stress – theoretical distribution and origin [13].

The residual stress introduced in the structural element results from the fabrication process, transportation and from other processing conditions. Due to a non-uniform cooling process, the

intersection zone from web and flange will shrink after the other zones and some plastic flow will be induced.

The hole drill method covers the procedure for determining residual stresses near the surface of isotropic linearly-elastic materials [14]. The use of special strain gauges will be necessary and a mechanical interference will be introduced into the specimen. The requirement of keeping the disturbance as small as possible is a positive factor in this method. The drill hole rosette shown in the figure 12 requires a small drill hole of about 1.5 [mm]. This can be regarded as a non-destructive technique [9] or as a “semi-destructive” because the damage that it causes is very localized and in many cases does not affect the usefulness of the specimen [14].

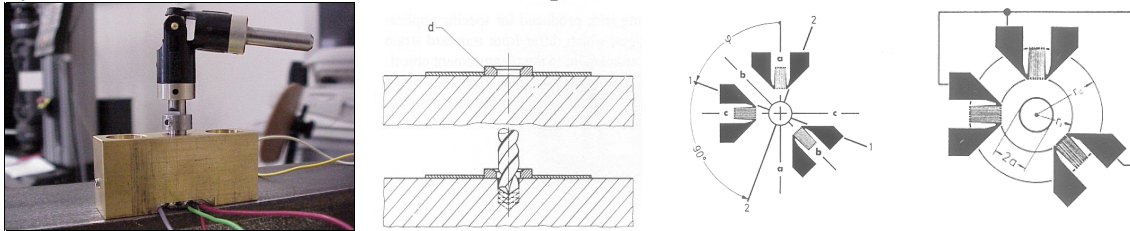


Figure 12: Residual stress measuring set-up with strain gauges rosette from HBM RY61.

The residual stresses were measured before and after the material being submitted to high temperature conditions. The objective of this experiment was to see if the stresses were relieved with the used temperature level. The residual initial stresses could be determined by the measured deformations  $\Delta\varepsilon_a$ ,  $\Delta\varepsilon_b$  and  $\Delta\varepsilon_c$  and by the elasticity theory, determined from the center of the flange, point of maximum residual stress value. In this experimental procedure a type A rosette [14] was used with the following dimensional geometric characteristics:  $a = 0.75$  [mm],  $r_1 = 1.8$  [mm],  $r_2 = 3.3$  [mm].

The principal directions “1” and “2” may be calculated with the simple formula (2), based on the measured strains, using a two-argument arctan function.

$$\varphi = \frac{1}{2} \arctg \left( \frac{\Delta\varepsilon_a + \Delta\varepsilon_c - 2\Delta\varepsilon_b}{\Delta\varepsilon_c - \Delta\varepsilon_a} \right) \quad \sigma_{1,2} = -\frac{E}{4A} (\Delta\varepsilon_a + \Delta\varepsilon_c) \pm \frac{E}{4B} \sqrt{(\Delta\varepsilon_a + \Delta\varepsilon_c - 2\Delta\varepsilon_b)^2 + (\Delta\varepsilon_c - \Delta\varepsilon_a)^2} \quad (2)$$

The results shown that the principal directions were align with the tested profile, as expected. The stresses may be computed form equation (2), considering that a tensile residual stress will produce negative relived strain and  $A$  and  $B$  may be calculated according to the geometric properties of this strain gauge and material properties [9]. The results before and after stress relief are presented in table 5, demonstrating that this type of methodology may reduce the internal and initial residual stresses in structural elements.

Table 5: Measured residual stresses and principal directions.

Specimen [°C]	Temperature [°C] / Dwell time [h] / Heat rate [°C/h]	$\sigma_1$ [MPa]	$\sigma_2$ [MPa]	$\varphi$	$\sigma_C$ [MPa]
Test 1	No	165,0	96,7	100	162,9
Test 2	No	191,0	121,0	109	183,6
Test 3	600 / 1 / 800	95,8	78,4	147	89,9

The stress  $\sigma_c$  represents the tension state in the flange along the profile direction. As represented in figure 11, a symmetric value should be expected in the web that should be responsible for the same amount of difference between tensile tests P18-P19 (see table 3) and P01-P04 (see table 1).

## 8 Conclusions

The material behavior after being submitted to elevated temperatures (fire conditions) depends essentially from the temperature level introduced into the structural element and from the cooling

process that may happen after accidental situation. If the material temperature exceeds the transition to austenitic phase a brittle material may be achieved, depending on the cooling process. In case of natural cooling the material will relief its residual stress  $\Delta\sigma_c$  in the some amount as the difference between the strength tensile tests, depending on the temperature level induced (550-650 [°C]). The hardness tests were done for all different studied cases, expecting higher results for brittle material. Two different scales were needed. The metallographic analysis is in accordance to the measured results.

The amount of stress relief is in agreement with the difference result of the tensile tests.

### Acknowledgments

This work was performed in the course of the research project PRAXIS/P/ECM/14176/1998, sponsored by the Portuguese Foundation for Science and Technology. Special thanks are due to the enterprise J. Soares Correia.

### References

- [1] Sanad, Moniem Abdel; *Behaviour of steel framed structures under fire condition* – British steel fire test1; research report R99-MD1; University of Edimburgh; December 1999.
- [2] Outinen, Jyri; Kaitila, Olli; Mäkeläinen; *High-temperature testing of structural steel and modeling of structures at fire temperatures* - Research report; Helsinki University of Technology laboratory of steel structures publications - TKK-TER-23; Espoo 2001.
- [3] Outinen, Jyri; Kesti, Jyrki; Mäkeläinen; *Fire Design Model for Structural Steel S355 Based Upon Transient State Tensile test results*; Journal Construct Steel Res.; Vol. 42, No.3, pp 161-169; 1997.
- [4] Pollack, Herman W.; *Materials Science and Metallurgy*; 4<sup>th</sup> edition, Prentice Hall – A reston book, 1988, USA.
- [5] CT12 – Instituto Português da Qualidade; *Norma Portuguesa NP 4072 – Materiais metálicos – Ensaio de dureza. Ensaio Rockwell (escalas HRBm e HR30Tm)*; Outubro 1990.
- [6] LNEC – Laboratório Nacional de Engenharia Civil; *Norma Portuguesa NP1467 – Aços e Ferros Fundidos – Preparação de provetes para metalografia*; Port. N° 321/77; Junho de 1977.
- [7] CT12 – Instituto Português da Qualidade; *Norma Portuguesa NP EN 10002-1 – Materiais metálicos – Ensaio de tracção. Parte 1: Método de ensaio (à temperatura ambiente)*; Novembro 1990.
- [8] Owens, Graham W.; Knowles, Peter R.; *Steel Designers Manual*; The Steel Construction Institute; 5<sup>th</sup> edition; Blackwell Scientific Publications, GB, 1992.
- [9] Hoffman Karl; *An introduction to measurements using strain gages*; HBM publisher; Germany; 1989.
- [10] Rubert A.; Schumann P.; *Temperaturabhängige Werkstoffeigenschaften von baustahl bei Brandbeanspruchung*; Stahlbau; Verlag Wilh. Ernst & Sohn; Berlin; 54; Heft 3; 81-86; 1985.
- [11] ECS ENV 1993-1-2; *Eurocode 3 – Design of steel structures – Part 1-2: General rules – Structural fire design*; 1995.
- [12] Franssen, J.M.; *Etude du comportement au feu des structures mixtes acier béton*, Thèse de doctorat; Collection de la F.S.A. ; N°111; Univ. de Liège, Belgium.
- [13] ESDEP Society; *European Steel Design Education Programme*; UK; CD-Rom version; 1999.
- [14] ASTM – Committee E28.13; *Standard Test Method for determining Residual Stresses by the Hole Drilling Strain Gage Method*; E837-01; USA; January 2002.
- [15] Dalton, William; *The Technology of Metallurgy*; Maxwell Macmillan International; USA; 1994.